DOI: https://doi.org/10.68732/fd56356076164381

ISBN: 978-9989-2053-6-1

Artificial fracture generation and surface roughness quantification in brittle rocks

T. Nikiema, N. Gonze, JP. Tshibangu & F. Descamps
University of Mons, Faculty of Engineering, Mons, Belgium
tegawende.nikiema@umons.ac.be
0000-0003-2079-2087

Abstract

Understanding the mechanical behaviour of rock masses is essential for the design and stability of infrastructures such as tunnels, slopes, and underground storage facilities. At these scales, discontinuities largely govern the global response of the rock mass. To investigate their behaviour, researchers typically adopt two approaches: working on natural fractures or on artificial ones. Natural fractures provide realistic conditions but pose significant challenges, both in terms of sampling and reproducibility. Artificial fractures, on the other hand, offer better control. They can be either molded from natural fracture surfaces, preserving geometry but losing the original rock nature and behaviour, or generated directly in the laboratory, which risks damaging the specimen. In this study, we focus on producing laboratory-induced fractures under controlled conditions to maintain the integrity of the rock.

Fracture initiation and propagation depend on the loading conditions, the mechanical properties, and the mineralogical composition of the rock. In this work, to produce fractures that preserve the morphology of natural rock splinters, an original methodology is developed to generate tensile fractures in rock samples using a 285 kN compression frame equipped with a blade-jaw system. This setup was tested on prismatic specimens of Soignies Limestone and Vosges Sandstone. These two rocks exhibit brittle behaviour under atmospheric conditions but differ markedly in porosity, stiffness, and strength (high to moderate), leading to distinct fracture patterns.

Optical profilometry is used to accurately characterize the geometry of fracture surfaces. Statistical roughness parameters and the Joint Roughness Coefficient (JRC) were used to quantify and compare the surface roughness of both rocks and assess the variability of laboratory generated fractures.

The methodology will play a key role in future work that will focus on linking joint geometry with the mechanical response of fractured rocks under controlled loading conditions.

Keywords

Laboratory-induced fractures, Soignies Limestone, Vosges Sandstone, Statistical roughness parameters, Joint Roughness Coefficient (JRC).

1 Introduction

Rock mass behaviour is strongly controlled by the presence and geometry of discontinuities such as joints, fractures, and bedding planes. These discontinuities govern the mechanical response, deformation mechanisms, and hydraulic properties of rock masses and therefore play a critical role in the design and stability assessment of underground structures, slopes, and foundations. A key parameter controlling the mechanical behaviour of rock joints is surface roughness, which influences shear strength, dilation, and contact mechanics.

Experimental investigation of joint behaviour requires representative fracture surfaces. In the literature, some have focused on understanding the mechanical behaviour of natural rock fractures (Schneider 1976; Krahn and Morgenstern 1979; Bandis et al. 1983; Huang et al. 1993), but their sampling is often difficult. In addition, natural fractures exhibit significant variability in geometry (roughness, orientation, and dipping), imbrication or opening, overlapping, filling materials, and weathering conditions. These factors make systematic laboratory investigations challenging. To overcome these limitations, artificial fractures are often generated in a laboratory to reproduce joint surfaces under controlled conditions. Several approaches have been used for this purpose, including sawing (Krahn and Morgenstern 1979), molding of natural surfaces (Schneider 1976), controlled splitting (Giwelli et al. 2009), or hydraulic fracturing (Huang et al. 1993). More recently, additive manufacturing techniques have been used to reproduce rock joints (Jaber 2020). While these methods allow the production of discontinuities, they often suffer from limitations such as unrealistic surface morphology, poor reproducibility, or alteration of the rock microstructure.

Establishing reproducible laboratory methods that yield realistic and complementary fracture surfaces remains an open challenge. In this context, the current study investigates a controlled fracturing technique using a blade-jaw system. The method aims to generate complementary fracture surfaces in prismatic rock samples while minimizing material loss and preserving surface morphology, under repetitive conditions. Two lithologies with contrasting mechanical and petrophysical properties were selected to evaluate the robustness of the method: Soignies Limestone and Vosges Sandstone.

The fracture surfaces are then characterized using optical 3D profilometry to quantify surface morphology. Statistical roughness parameters and Joint Roughness Coefficient (JRC) values are derived from surface profiles to evaluate surface characteristics and directional variability.

2 Methods

2.1 Sample description

Two rock types were selected for this study: Soignies Limestone (SL) and Vosges Sandstone (VS), chosen for their availability, relative homogeneity, and contrasting mechanical properties. Soignies Limestone is a compact rock with a porosity of 0.4% and a high compressive strength (UCS typically ranging between 100 and 125 MPa). It consists mainly of $CaCO_3$ (>95%) and displays a micritic texture (Descamps et al. 2011). In contrast, Vosges Sandstone is more porous (≈22%), moderately strong (UCS≈40 MPa), with a granular texture (100 – 150 μm) and a silica content ranging from 70 to 95% (Descamps 2007). Under atmospheric conditions, both rock types exhibit elastic–brittle behaviour (Descamps 2007, Descamps et al. 2011). As sedimentary rocks, both contain bedding planes, but their mechanical behaviour can be considered isotropic.

2.2 Artificial fracture generation

Fracturing was performed using a blade–jaw system (Fig. 1a). The device consists of two tungsten steel blades (10 cm long) forming a loading jaw. The blade tips are V-shaped and fit into pre-machined grooves in the specimen. The upper blade slides along two guiding columns and is connected to a loading platen that applies the load. A ball joint incorporated into the upper platen ensures uniform load distribution along the blade–specimen contact. The lower blade is in contact with a lower platen transmitting the applied load.

The overarching research objectives aim to address the mechanical behaviour of fractures by performing compression and direct shear tests. Particularly for shear tests, ISRM recommendations and ASTM standards provide guidelines for the general sample geometry (Ulusay 2015; ASTM D18 Committee 2017). Coupled with practical constraints of the laboratory, the sample size for the current

study was defined to allow subsequent mechanical testing, with dimensions of 95 × 60 × 60 mm. The fracture surface corresponds to the 95 × 60 mm section.

Lateral grooves (3–4 mm deep) were machined along the edges to initiate and guide fracture propagation, resulting in a slightly reduced effective fracture area. Guiding the fracture in the middle of the block was also necessary to allow further compression and direct shear tests.

Fig. 1b illustrates a fractured surface wall, with a profilometric scan highlighting height variations of the surface.

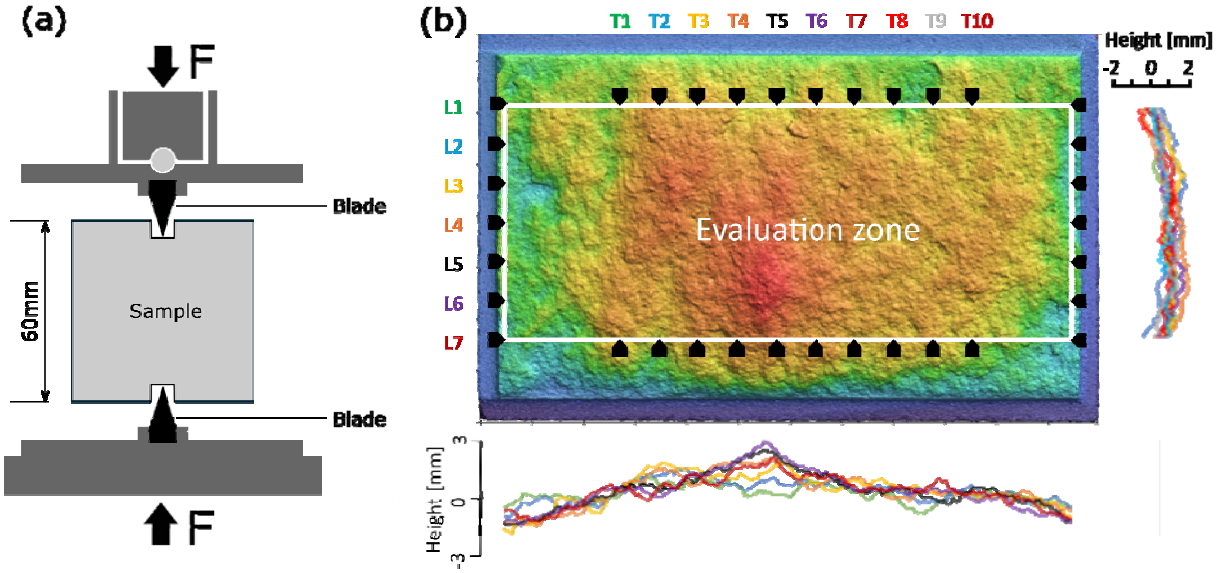


Fig. 1 a) Blade-jaw controlled fracturing system, F is the direction of controlled load application. b) Fracture surface wall with the evaluation area delineated by a white rectangular outline, and the positions of the profiles indicated by black arrows. Roughness profiles are traced in longitudinal and transversal directions.

2.3 Optical profilometric analysis of roughness

Fracture surface roughness was analysed using a Keyence VR-6200 3D optical profilometer, which measures surface topography through structured light projection. The instrument provides a spatial resolution of ±5 µm in the horizontal directions and ±4 µm in the vertical direction.

Each fracture wall was analysed separately. To reduce edge effects caused by the grooves and damage resulting from stress concentration near the blades, an evaluation zone was defined, excluding margins up to11 mm along the longitudinal edges and up to17.5 mm along the transversal edges (Fig. 1b). Within this zone, linear profiles were evenly distributed. Seven longitudinal profiles (L1–L7) with lengths ranging from 80 to 91 mm and ten transversal profiles (T1–T10) with lengths of about 38 mm were extracted. Roughness profiles traced in longitudinal and transversal directions overlap in each direction.

Four common statistical roughness parameters are computed for each profile (Tatone and Grasselli 2010; Nikiema et al. 2024): the absolute roughness (R_z), the arithmetic roughness (R_a), the root mean square slope (Z_2), and the linear roughness (R_L) or roughness profile index (R_p). Z_2 and $R_p$are correlated with Barton's Joint Roughness Coefficient (JRC), the most widely used roughness index in geomechanics for the assessment of rock mass stability. Eq.1 and Eq.2 were proposed by Nikiema et al.(2024):

$$JRC = 65.25Z_2 - 11.21 \qquad R^2 = 0.935 \qquad (1)$$

$$JRC = 238.6R_p - 240.57 \qquad R^2 = 0.924 \qquad (2)$$

3 Results

3.1 Analysis of fracture quality

Fifteen specimens of SL and seven specimens of VS were successfully split without any sample loss. The resulting fractures generally followed the predefined plane, with only minor local deviations, and

no unusable fracture surfaces were produced. Mass measurements performed before and after fracturing indicate a very limited material loss, ranging from 0 to 4 mm³/cm² over the fractured area for both rock types. Moreover, most of the fractured samples show complementary walls that fit closely together, indicating that the fracturing process preserves the morphological correspondence between the two sides of the joint.

As expected, the linear splitting load is higher for SL than for VS, with mean values of 21 N/mm (coefficient of variation (CV): 21.79%) and 9 N/mm (CV: 6.15%), respectively. This difference reflects the contrasting mechanical behaviour.

The fracture morphology varies with rock type. In VS, fracturing appears predominantly intergranular, which is consistent with its granular grain size. In contrast, SL is characterized by a micritic texture and mainly exhibits fracture propagation through the matrix.

3.2 Surface roughness by optical profilometry

Five specimens of each rock were randomly selected for detailed analysis. Three longitudinal and four transversal profiles were extracted per wall to ensure representative coverage. Lower wall roughness values were plotted against upper wall values to evaluate morphological correspondence relative to a 1:1 identity line (Fig. 2). The upper and lower walls were randomly assigned to each specimen.

In the longitudinal direction and for both rocks, amplitude parameters (R_a,R_z) exhibit an excellent fit (R^2: $0.97 - 1.00$), demonstrating strong linear correlation between paired fracture walls. Slope and profile index parameters (Z_2,R_p) show moderate linear correlation (R^2: $0.60 - 0.70$) due to relatively compact clusters around the correlation line. This morphological agreement is validated by Lin's concordance coefficient ($CCC > 0.90\ for\ R_a\ and\ R_z$, except for R_z in SL ($CCC = 0.79$). The relative quadratic error from the 1:1 identity line remains low ($0\,\% - 3\,\%$ for SL ; $1\,\% - 11\,\%$ for VS), confirming that absolute deviations are minor and that roughness variability between corresponding walls is limited.

The transversal direction displays a more pronounced dispersion. For R_a, SL data are asymmetric with most points located in the upper triangular region and scattered ($\mathrm{CCC} = 0.66, \mathrm{error}: 24\,\%$), whereas VS data are more evenly distributed despite a low concordance ($\mathrm{CCC} = 0.17, \mathrm{error}: 66\,\%$). Conversely, R_z maintains high correlation ($R^2 \geq 0.98$) and good concordance ($\mathrm{CCC}: 0.74 - 0.85, \mathrm{error}: 15\,\% - 16\,\%$), indicating that peak-to-valley amplitudes are corresponding between the fracture walls. Although Z_2 and R_p yield very low relative quadratic errors (1 %), they exhibit low concordance (CCC<0.40) due to highly clustered data points, reflecting local slope disparities. Local deviations observed for specimens SL14, VS26, and VS29 are linked to local discrepancies, such as an intact fossil shell in SL14. Furthermore, transversal profiles are much shorter than longitudinal ones. This may amplify the observed differences.

JRC was computed from Z_2 and R_L, using Eq. 1 and 2. For longitudinal profiles, JRC ranges from 6 to 9 for SL (mean: 7, CV: 11 %), and from 10 to 12 for VS. Transversally, JRC ranges from 6 to 15 for SL (mean: 9, CV: 25 %), and from 11 to 15 for VS (mean: 12, CV: 10 %).

To assess the representativeness of the laboratory-induced surfaces, these results were compared with those obtained from eight natural fracture surfaces (Table 1). Most parameters fall within the range measured on laboratory-induced fractures, except R_z, which reaches higher values on natural surfaces, indicating a great amplitude difference in natural surfaces.

Finally, comparing longitudinal and transversal profiles (Fig. 2i and j) shows that the distribution of data points is not correlated between the two measurement directions, indicating directional heterogeneity in fracture surface roughness.

Table 1. Measurements of roughness on natural fractures for both rock types.

Rock type	$\boldsymbol{R_a}[\mu\boldsymbol{m}]$	$\boldsymbol{R_z}\ [\mu\boldsymbol{m}]$	$\boldsymbol{Z_2}\ [-]$	$\boldsymbol{R_p}\ [-]$
Soignies Limestones	1356 ± 227	6341 ± 1437	0.340 ± 0.036	1.051 ± 0.009
Vosges Sandstones	524 ± 125	2588 ± 366	0.293 ± 0.015	1.039 ± 0.003

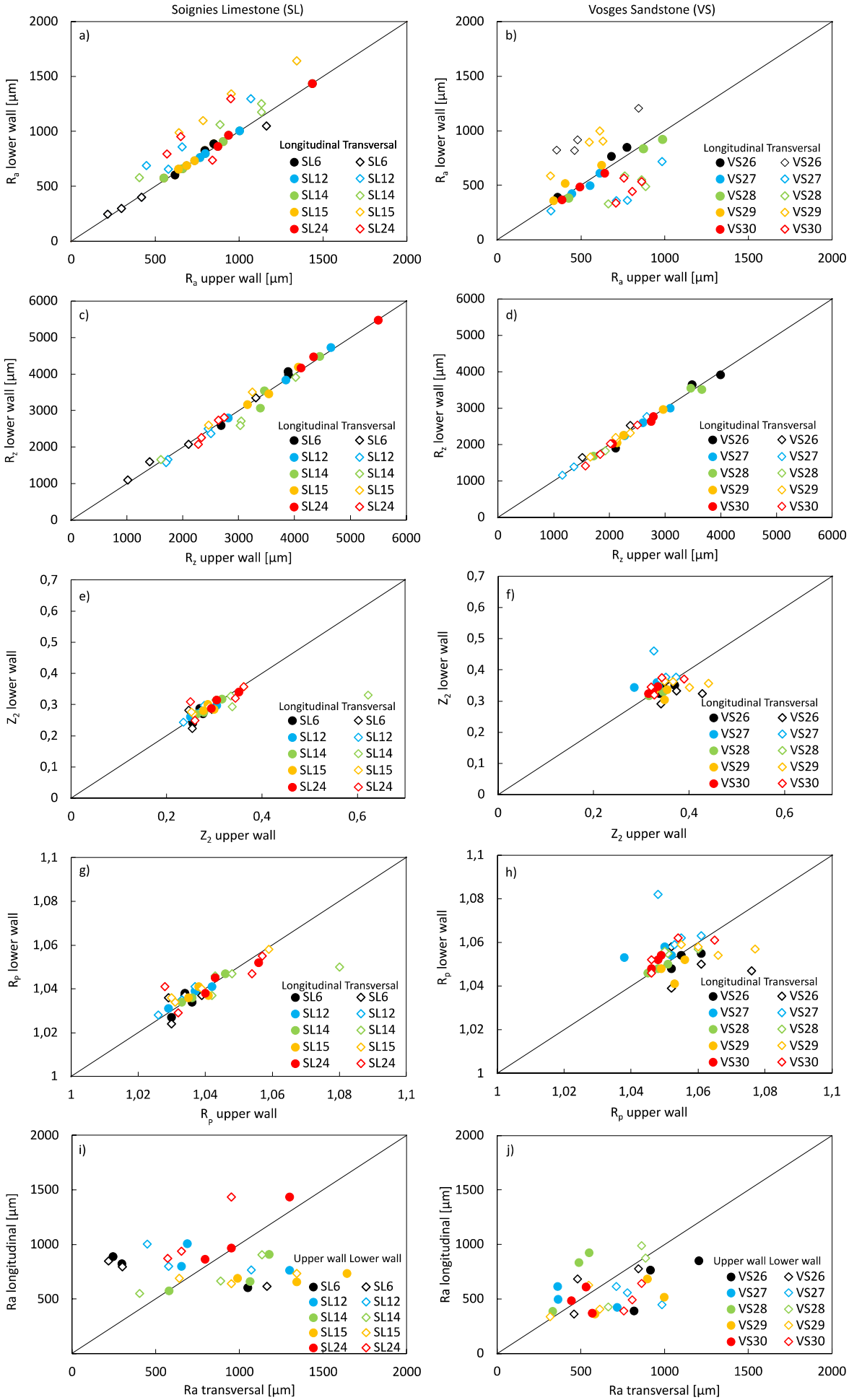


Fig. 2 Relationships between the roughness parameters (R_a, R_z, Z_2, R_p) measured on the two corresponding fracture walls for Soignies Limestone (a, c, e, g,i) and Vosges Sandstone (b, d, f, h, j) in both longitudinal and transversal directions.

4 Conclusion

This study presented an experimental method for generating artificial fractures in rock specimens using a blade-jaw controlled system. Soignies Limestone and Vosges Sandstone, which feature contrasting petrophysical and mechanical properties, were investigated to assess the method's applicability. Surface quality analysis shows that the fracture mostly follows the predefined plane imposed by the grooves, with very limited material loss.

Optical profilometry was used to characterize roughness parameters both on longitudinal and transversal profiles. The results are consistent with roughness parameters measured on natural fractures for the same rocks.

Nevertheless, several limitations remain. The influence of experimental parameters, such as loading rate and groove geometry, has not been thoroughly investigated. Further work should combine the geometric characterization of fracture surfaces with mechanical testing to establish quantitative relationships between roughness parameters and joint mechanical behaviour.

References

ASTM D18 Committee (2017) "D5607 - 16 Test Method for Performing Laboratory Direct Shear Strength Tests of Rock Specimens Under Constant Normal Force." ASTM International. DOI: 1520/D5607-16.

Bandis, S.C., Lumsden, A.C. and Barton, N.R. (1983) "Fundamentals of Rock Joint Deformation," International Journal of Rock Mechanics and Mining Sciences & Geomechanics, Vol 20(No 6), pp. 249–268.

Barton, N. (1973) "Review of a new shear-strength criterion for rock joints," Engineering Geology, 7, pp. 287–332.

Descamps, F.(2007) Étude du comportement des roches poreuses saturées aux conditions de grande profondeur. Thèse de doctorat. Service de Génie Minier - Faculté Polytechnique de Mons - Université de Mons.

Descamps, F.,Tshibangu, JP., Da Silva, M., Schroeder, C., Verbrugge, J.(2011) "Behaviour of carbonated rocks under true triaxial compression," in Y. Zhou (ed.) Harmonising Rock Engineering and the Environment. CRC Press, pp. 597–602. DOI: 10.1201/b11646-105.

Giwelli, A.A., Sakaguchi, K. and Matsuki, K. (2009) "Experimental study of the effect of fracture size on closure behavior of a tensile fracture under normal stress," International Journal of Rock Mechanics and Mining Sciences, 46(3), pp. 462–470. DOI: 10.1016/j.ijrmms.2008.11.008.

Huang, X. et al. (1993) "An investigation of the mechanics of rock joints—Part I. Laboratory investigation," International Journal of Rock Mechanics and Mining Sciences & Geomechanics Abstracts, 30(3), pp. 257–269. DOI: 10.1016/0148-9062(93)92729-A.

Jaber, J. (2020) Application de la fabrication additive à la modélisation physique des joints et des massifs rocheux, par approches expérimentales et numériques. Thèse de doctorat. Université de Lorraine. Available at: https://hal.univ-lorraine.fr/tel-02960385v1 (Accessed: March 25, 2023).

Krahn, J. and Morgenstern, N.R. (1979) "The ultimate frictional resistance of rock discontinuities," International Journal of Rock Mechanics and Mining Sciences & Geomechanics, 16(2), pp. 127–133. DOI: 10.1016/0148-9062(79)91449-9.

Nikiema, T., Gonze, N. and Descamps, F. (2024) "Correlation between Joint Roughness Coefficient (JRC) and statistical roughness parameters," Engineering Geology and Geotechnics: Building for the Future, Proceedings of the Conference EUROENGEO 2024. 4th European Regional Conference of IAEG, University of Zagreb Faculty of Civil Engineering, pp. 135–142. DOI: 10.5592/CO/EUROENGEO.2024.203.

Schneider, H.J. (1976) "The friction and deformation behaviour of rock joints," Rock Mechanics Felsmechanik Mecanique des Roches, 8(3), pp. 169–184. DOI: 10.1007/BF01239813.

Tatone, B.S.A. and Grasselli, G. (2010) "A new 2D discontinuity roughness parameter and its correlation with JRC," *International Journal of Rock Mechanics and Mining Sciences*, 47(8), pp. 1391–1400. DOI: 10.1016/j.ijrmms.2010.06.006.

Ulusay, R. (ed.) (2015) The ISRM Suggested Methods for Rock Characterization, Testing and Monitoring: 2007-2014. Cham: Springer International Publishing. DOI: 10.1007/978-3-319-07713-0.